Asian Journal of Chemistry Vol. 22, No. 7 (2010), 5428-5442

Fabrication and Characterization of Photoelectrocatalytic Electrodes of Carbon Nanotube/Titanium Oxide

WON-CHUN OH*, FENG-JUN ZHANG† and MING-LIANG CHEN
Department of Advanced Materials & Science Engineering,
Hanseo University, Chungnam 356-706, South Korea
Fax: (82)(41)6883352; Tel: (82)(41)6601337; E-mail: wc_oh@hanseo.ac.kr

In this paper, we have prepared three types of carbon nanotube/titanium oxide (CNT/TiO_2) electrodes (designated as SCTE1, SCTE2 and SCTE3). The electrodes prepared were characterized by surface properties, structural crystallinity, elemental identification and photoelectrocatalytic activity. Nitrogen adsorption data showed that the composites had decreased surface area compared with pristine CNTs, indicating blocking of micropores on the CNT surfaces, which was further supported by observations *via* SEM. XRD patterns of the composites showed that the SCTE 1 composite contained only a typical single and clear anatase form while the SCTE2 and SCTE3 contained a mixture of anatase and rutile phases. EDX spectra showed the presence of C, O and Ti peaks for all samples. The catalytic efficiency of the electrodes prepared was evaluated by the photoelectrodegradation of methylene blue. The positive potential applied in photoelectrocatalytic oxidation was studied. It was found that photoelectrocatalytic decomposition of methylene blue could be attributed to the synthesized effects of TiO_2 photocatalytic, CNT electro-assisted and as function of applied potential. The efficiency of photoelectrocatalytic oxidation for methylene blue is higher than that of photocatalytic oxidation. A degradation mechanism is presented.

Key Words: CNT/TiO_2 electrode, Photoelectrocatalysis, XRD, SEM, Methylene blue.

INTRODUCTION

In the last decade, as one of the most promising candidate photocatalysts for application in environmental protection and water treatment, titania has attracted great attention from scientists and engineers from the view point of practical application because of its high stability against photocorrosion, high photocatalytic (PC) activity, low cost and its environmental non-toxicity[1]. The application form of TiO_2 as a photocatalyst seems to have the following two main ways: particle and electrode. However, a high cost and low efficiency for the particle-fluid separation process after radiation treatment for the reuse of the catalyst restrained its industrial applications[2]. Therefore, development of TiO_2 photocatalysts immobilized on a certain

†Anhui Key Laboratory of Advanced Building Materials, Anhui University of Architecture, Anhui, Hefei 230022, P.R. China.

suitable adsorbent such as activated carbon would be of great significance, not only to avoid the disadvantages of the filtration process of fine photocatalyst particles, but also to lead to high photodecomposition efficiency[3,4].

Briefly, a photocatalytic method is based on the reactive properties of photo-generated electron-hole pairs. They are generated in the semiconductor (TiO_2) particles under UV irradiation, at the same time these electrons and holes could also recombine. Since the hole is a powerful oxidizing agent, it could decompose water and/or contaminants adsorbed on the TiO_2 surface. In comparison, in a photoelectrocatalytic (PEC) method, a positive potential is applied on the working electrode, which inhibits the recombination of electrons and holes and, therefore, enhances the rate of PEC degradation of organic compounds[5-7]. There were many reports on PEC degradation of organic pollutants using TiO_2 electrodes. Christensen *et al.*[8] have reported that 'sol-gel' electrodes were made by depositing and then heating a layer of titania gel on titanium mesh for the PEC and PC disinfection of *E. coli* suspensions. The photo-degradation of humic acid (HA) in an aqueous solution by PEC oxidation using a Ti/TiO_2 mesh electrode has been investigated[9]. Jiang *et al.*[10] have studied the photocatalytic oxidation kinetics of adsorbed organic compounds at particulate TiO_2 film electrodes. Zhang *et al.*[11] have reported that mesoporous TiO_2 film photocatalysts supported on stainless steel substrates were prepared using a sol-gel method with $Ti(OC_4H_9)_4$ as a precursor and polyethylene glycol as a structure-directing agent.

The common characteristics of the above TiO_2 electrodes are the immobilization of TiO_2 on a titanium mesh or a stainless steel surface. According to previous studies[12-15], carbon-TiO_2 composites, especially CNT/TiO_2 composites, have a high surface area, porous texture distribution and showed an excellent photoactivity[16,17]. Therefore, carbon nanotubes (CNT) have been proposed as a promising candidate as the support materials for TiO_2 catalyst depositions.

In this study, we focused on the fabrication and characterization of the CNT/TiO_2 composite electrodes in a composite process. The pre-oxidized CNT were mixed with different concentrations of titanium *n*-butoxide (TNB, $Ti(OC_4H_7)_4$) solution and formed CNT/TiO_2 gels, through molding and pressing after the addition of phenol resin, followed by heat treatment, CNT/TiO_2 composite electrodes were prepared. The prepared electrodes were characterized by BET surface area, X-ray diffraction (XRD), a scanning electron microscope (SEM), energy dispersive X-ray spectroscope (EDX). The catalytic efficiency of the electrodes developed was evaluated by the photoelectrodegradation of an azo compound, methylene blue (MB, $C_{16}H_{18}N_3S{\cdot}Cl{\cdot}3H_2O$).

EXPERIMENTAL

Carbon nanotubes supplied from the carbon nano-material technology Co., Ltd, Korea. (multiwall nanotubes, diameter: *ca.* 20 nm, length: *ca.* 5 μm), were used without further purification. Titanium *n*-butoxide ($Ti(OC_4H_7)_4$) as a titanium source for the preparation of CNT/TiO_2 composites was purchased from Acros Organics,

New Jersey, USA. For the oxidization of the surfaces of CNT, *m*-chloroperbenzoic acid (MCPBA) was used as an oxidized reagent which was purchased from Acros Organics, New Jersey, USA. Benzene (99.5 %) was used as an organic solvent which was purchased from Samchun Pure Chemical Co., Ltd, Korea. The novolac typed phenol resin was supplied from Kangnam Chemical Co., Ltd, Korea. Methylene blue was used as analytical grade which was purchased from Duksan Pure Chemical Co., Ltd, Korea. It was selected because it can readily under anaerobic conditions produce potentially more hazardous aromatic amines.

Preparation of CNT/TiO_2 electrodes: In these experiments, at first, to prepare the oxidizing agent, 2.0 g *m*-chloroperbenzoic acid (MCPBA) was melted in 60 mL benzene. Then 0.6 g CNT was put into the oxidizing agent, refluxed for 6 h, filtered and dried. The oxidized CNT was put into the mixed solution of titanium *n*-butoxide and benzene with different volume ratios. Then the solutions were homogenized under refluxing at 343 K for 5 h using a magnetic stirrer in a vial. After stirring the solutions were transformed to the CNT/TiO_2 gels and these gels were heat treated at 973 K for 1 h with a heating rate of 279 K/min. Then 0.4 g phenol resin was added into these CNT/TiO_2 composites, the composites were pressed at a pressure of 25 MPa in a mould, whose dimensions were 9.95 mm × 39.5 mm × 5.95 mm. These were then heat treated at 673 K for 1 h and the CNT/TiO_2 electrodes were prepared. The preparation conditions and code of samples are listed in Table-1.

TABLE-1
NOMENCLATURES OF CNT/TiO_2 ELECTRODE

Preparation method	Nomenclatures
MCPBA + CNT + (TNB 2 mL + benzene 18 mL) + phenol resin	SCTE1
MCPBA + CNT + (TNB 4 mL + benzene 16 mL) + phenol resin	SCTE2
MCPBA + CNT + (TNB 6 mL + benzene 14 mL) + phenol resin	SCTE3

Characteristics and investigations of the samples: The Brunauer-Emett-Teller (BET) surface area of the CNT/TiO_2 composites was evaluated from N_2 adsorption isotherms at 77 K using a BEL Sorp Analyzer (BEL, Japan). XRD was used for crystal phase identification and estimation of the anastase-to-rutile ratio. XRD patterns were obtained at room temperature with a diffractometer Shimata XD-D1 (Japan) using CuK_α radiation. SEM was used to observe the surface state and porous structure of the CNT/TiO_2 composites using a JSM-5200 JOEL electron microscope (Japan). EDX was used to measure the elemental analysis of the CNT/TiO_2 composites. UV-Vis spectra for the MB solution degraded by CNT/TiO_2 composite dispersions under different conditions were recorded using a Genspec III (Hitachi, Japan) spectrometer.

Photoelectrocatalytic (PEC) decompositions: The PEC decomposition was performed using a CNT/TiO_2 electrode in a 100 mL glass container and then irradiating the system with 20 W UV light at 365 nm, which was used at a distance of 100 mm from the solution in a dark box. The counter electrode was artificial graphite (TCK,

Korea, 9.95 mm × 39.5 mm × 5.95 mm in size). The same CNT/TiO_2 electrode was placed in 50 mL of 1.0×10^{-5} mol/L MB solution. The PEC degradation of MB was performed with a voltage of 6.0V and UV light. The PEC activities of the CNT/TiO_2 electrodes were investigated using the PEC rate of MB, which was measured as function of time. The blue colour of the solution faded gradually with time due to the adsorption and decomposition of the MB. Also the concentration of MB in the solution was determined as a function of irradiation time from the absorbance change at a wavelength of 660 nm.

RESULTS AND DISCUSSION

Structure and morphology of CNT/ TiO_2 composites: Nitrogen adsorption isotherms and pore size distributions for pristine CNT and CNT/TiO_2 composites are shown in Figs. 1 and 2. Fig. 1 shows an idealized form of the adsorption isotherm for physisorption on CNT/TiO_2 composites. The formation of type II (classified with an IUPAC) adsorption isotherms confirmed a mixed micro- and mesoporous texture. The values of BET surface area of CNT/TiO_2 composites are shown in Table-2. From the results of Table-2, the BET surface areas of pristine CNT was 232.2 m^2/g, while the BET surface areas of the SCTE series composites decreased gradually from 228.5 to 166.9 m^2/g with an increase of the TNB concentration. This demonstrated that there is a decrease in the BET surface area of the CNT/TiO_2 composites after the formation of TiO_2 particles by the TNB treatment, which suggests that some porosity was developed during the heat treatment. However, the micropore volume of the CNT/TiO_2 composites decreased from 0.8 to 0.3 cm^3/g with an increase of the TNB concentration. The average pore diameter of SCTE1, SCTE2 and SCTE3 were 11.7, 8.0 and 6.5 (nm), respectively. It was considered that the composites are mainly nano materials including many micro-pores. It was considered that there are two reasons for this. First, this could be attributed to the partial blocking of micropores by the formation of TiO_2 on the CNT surface with the heat treatment. Second, the BET surface area decreased due to the curing of the polymer resin by heat treatment, which blocked the micropores and formed some new mesopores. It was possible that the phenol resin had coated some CNT particles to form some larger composite particles during the curing process. The same phenomena can be well confirmed by the SEM observations of the morphology of CNT/TiO_2 composites. In addition, as shown in Fig. 2, there were two peaks formed around 1 nm and 11 nm for the three types of samples of CNT/TiO_2 composites, respectively. Moreover, the intensity of these peaks became gradually weaker with an increase of the TNB concentration. It can be seen that there was more change in the micropore size distribution of CNT/TiO_2 composites compared than that of pristine CNT. This result indicated that the total surface area decreased in the process of TiO_2 formation on the CNT surface and that the normal pore structure was destroyed at the same time. As expected, the BET surface area is thought to decrease due to the blocking of the micropores by surface complexes introduced through the formation of CNT/TiO_2 composites.

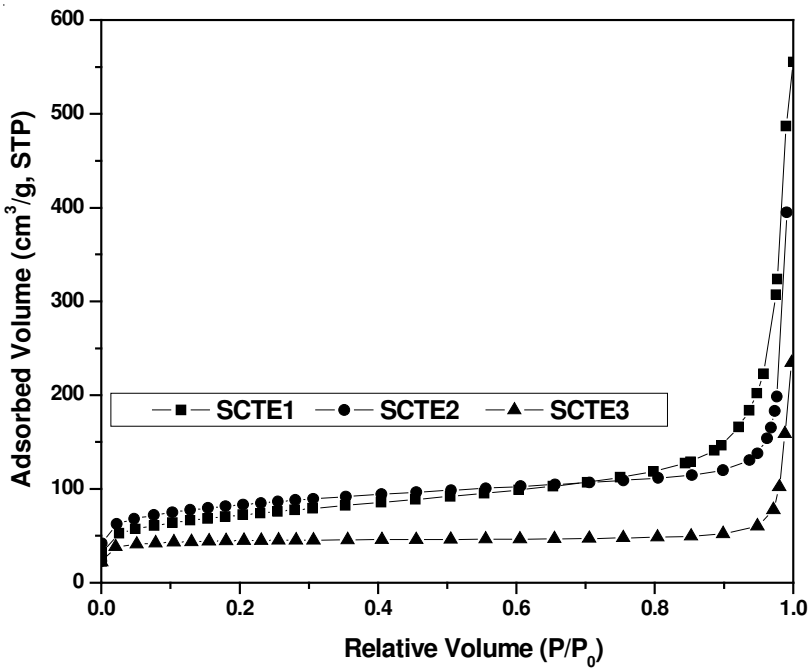

Fig. 1. Adsorption isotherms of N_2 at 77 K on the pristine materials and CNT/TiO_2 composites

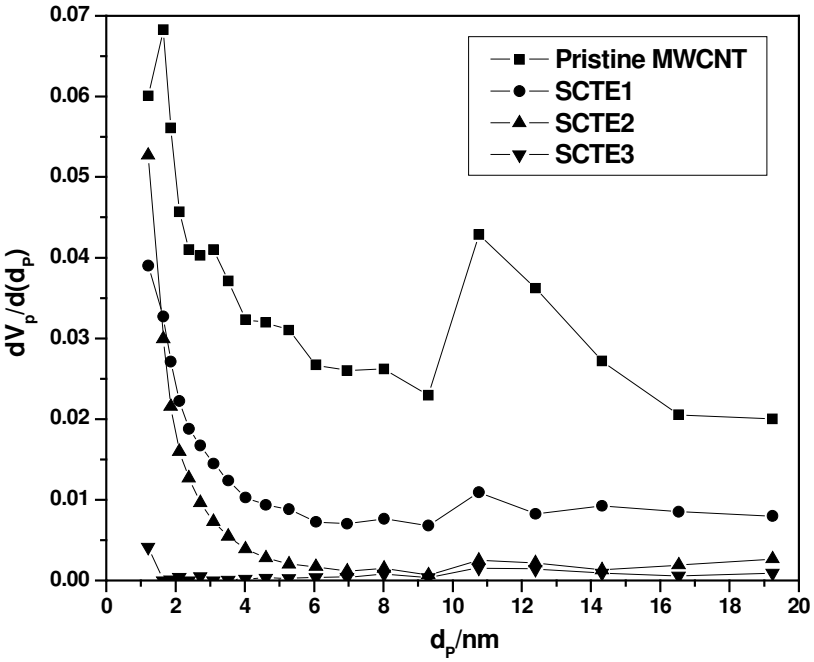

Fig. 2. Comparison of pore size distribution for the pristine CNT and CNT/TiO_2 composites

TABLE-2
TEXTURAL PROPERTIES OF ORIGINAL MWCNT AND CNT/TiO_2 COMPOSITE SAMPLES

Sample	Parameter		
	SBET (m^2/g)	Micropore volume (cm^3/g)	Average pore diameter (nm)
Original MWCNT	232.2	0.6	9.5
SCTE1	228.5	0.8	11.7
SCTE2	198.4	0.6	8.0
SCTE3	166.9	0.3	6.5

The XRD results for the catalyst samples are shown in Fig. 3. The structure of SCTE1 showed a typical single and clear anatase crystal structure. With an increase of the TNB, however, the structure for SCTE 2 and SCTE3 showed a mixture of anatase and rutile crystals. It is well known that the crystal structure of titanium dioxide is mainly determined by the heat treated temperature. The samples were heated at 973 K for 1 h. The peaks at 25.3, 37.8, 48.0 and 62.5 are the diffractions from (101), (004), (200) and (204) planes of anatase, indicating the CNT/TiO_2 composites developed existed in an anatase state. The peaks at 27.4, 36.1, 41.2 and 54.3 belong to the diffraction peaks of (110), (101), (111) and (211) planes of rutile. Therefore, it can be concluded that the CNT/TiO_2 composites developed had a mixture of structures of anatase and rutile crystals. As we know, the anatase phase formed below 773 K starts to transform to rutile-type structure above 873 K and changed into single phase of rutile at 973-1173 K[18].The results are in accordance with reference[19], so the XRD results of SCTE2 and SCTE1 in this study are reasonable. For the SCTE1 after the heat treatment at 973 K for 1 h, however, the main crystalline phase has not transformed to the rutile structure. It is proposed that the crystalline phase transformation of TiO_2 was affected by the amount of TiO_2 and CNT except temperature.

The micro-surface structures and morphology of CNT/TiO_2 composites were characterized by SEM and FESEM. Fig. 4 shows the changes in the morphology of CNT/TiO_2 composites. As shown in Fig. 4, for all samples, TiO_2 particles were fixed on the surface of the CNT network in the forms of small clusters and the distribution was not uniform. These results were confirmed as well by FESEM inspection of CNT/TiO_2 composites which can be seen clearly in Fig. 4g and h. In Fig. 4b, d and f, it was also observed that the amount of clusters increased with an increase of the amount of TNB and that the size of TiO_2 particles became larger with an increase in the amount of TNB. It was considered that a good dispersion of small particles could provide more reactive sites for the reactants than aggregated particles. This is consistent with the Wang *et al.*[20,21] reports, that CNT introduced into TiO_2 can prevent TiO_2 particles from agglomerating. Therefore, the higher PC activity of the CNT/TiO_2 composites prepared might be attributed to photodegradation. At the same time, the conductive CNT network can facilitate the electron transfer

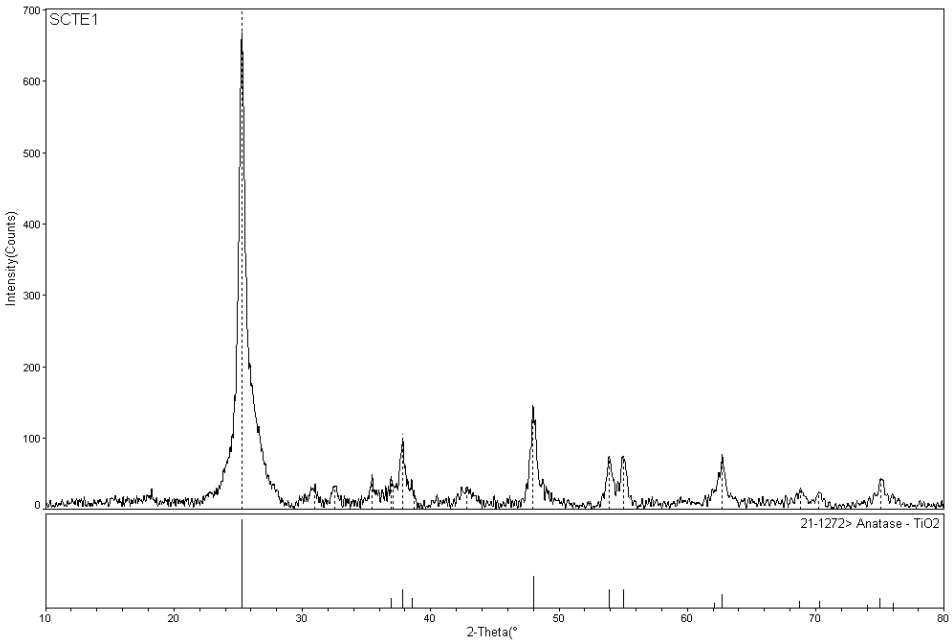

(a) SCTE1

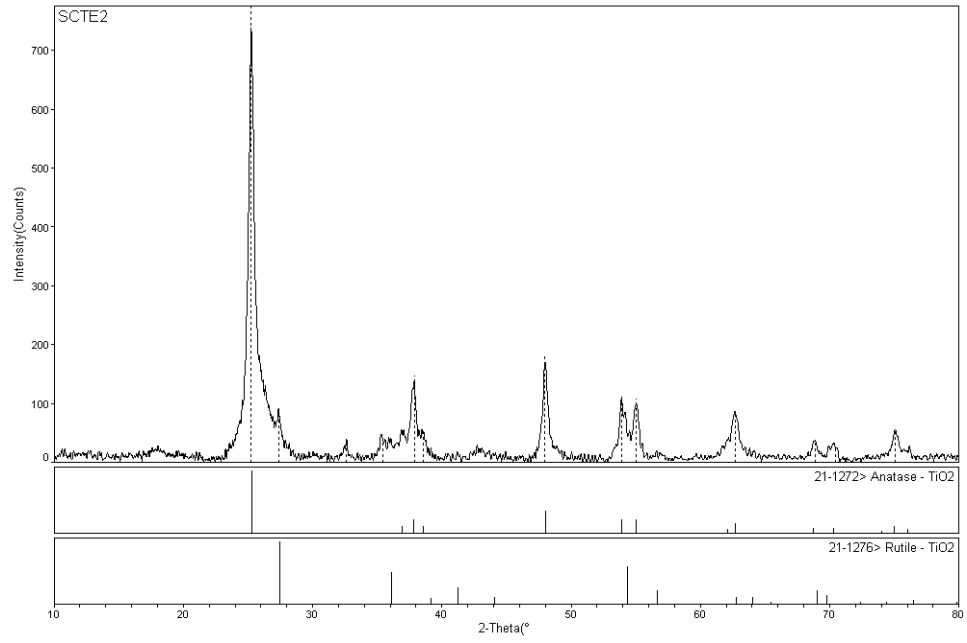

(b) SCTE2

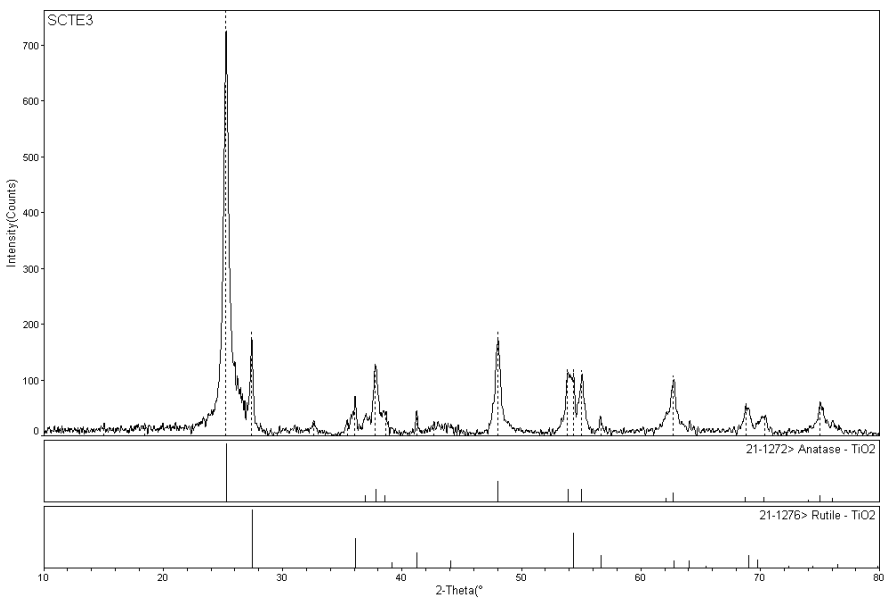

(c) SCTE3

Fig. 3. XRD patterns of CNT/TiO_2 composites (a) SCTE1, (b) SCTE2 and (c) SCTE3

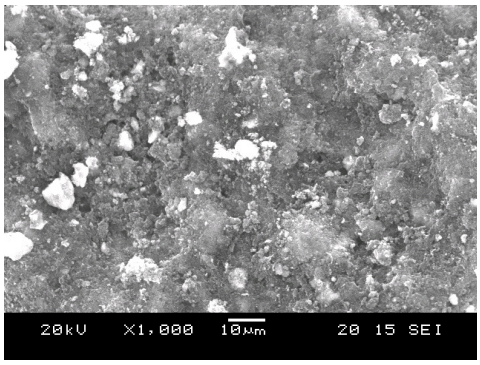

(a)

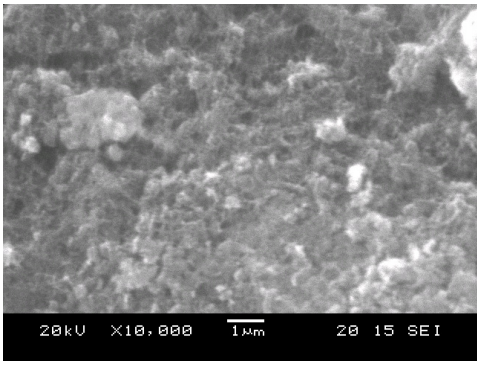

(b)

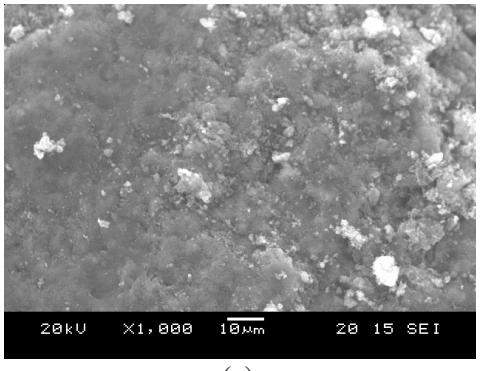

(c)

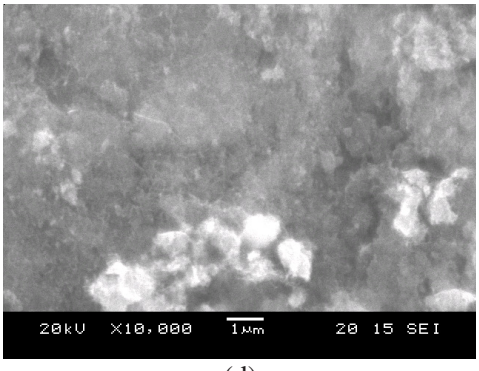

(d)

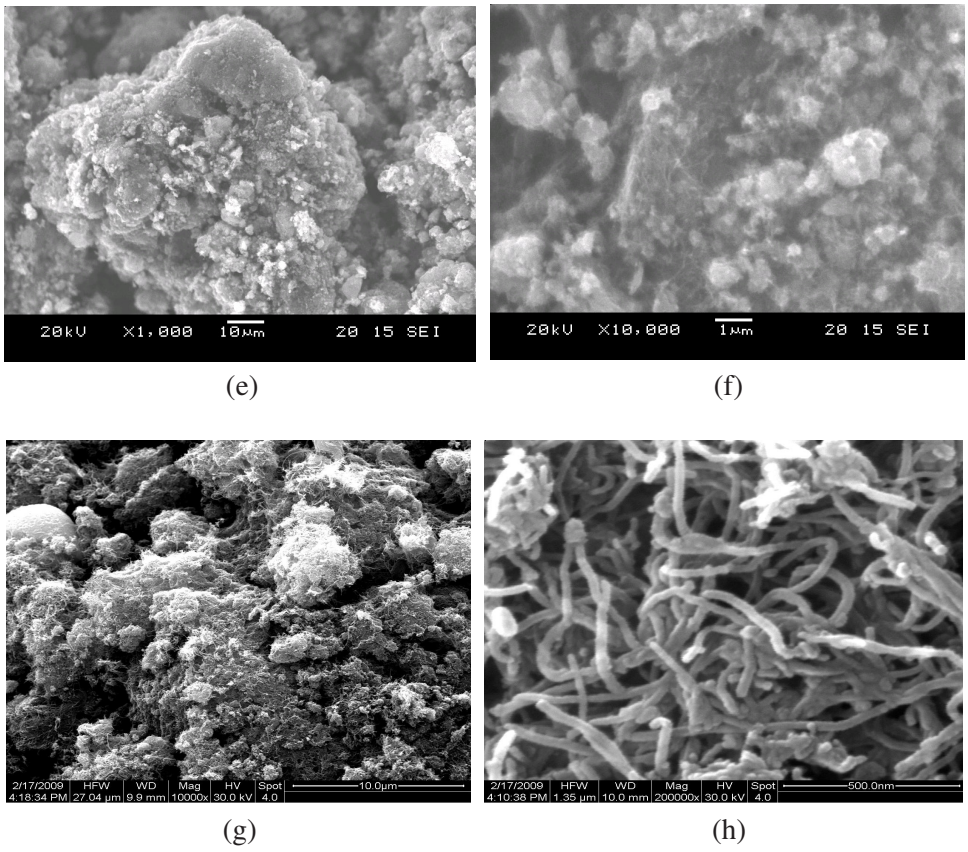

Fig. 4. SEM and FESEM images obtained from powdered CNT/TiO_2 composites: (a) SCTE1 (over-all scale), (b) SCTE1 (close-up), (c) SCTE 2 (over-all scale), (d) SCTE2 (close-up), (e) SCTE3 (over-all scale), (f) SCTE3 (close-up), (g) SCTE2, (h) SCTE2

between the adsorbed MB molecules and the catalyst substrate[8,22]. This will be beneficial for the PEC reaction because the PEC reaction is carried out on the surface of the CNT/TiO_2 composite catalysts and the CNT network. So the CNT/TiO_2 composites would show an excellent PEC activity.

Fig. 5 shows the EDX spectra of CNT/TiO_2 composites prepared. From the EDX data, the main elements such as C, O and Ti existed and other impurity elements were also existed (impurity elements derived from the CNTs). The results of EDX elemental microanalysis of CNT/TiO_2 composites are listed in Table-3. The Ti contents of SCTE1, SCTE2 and SCTE3 are 14.93, 21.69 and 30.64 %, respectively; as expected, the Ti element contents in the composites increased with an increase of the TNB concentration. It is proposed that an increase of the Ti content increases the photocatalytic activity for the decomposition of MB.

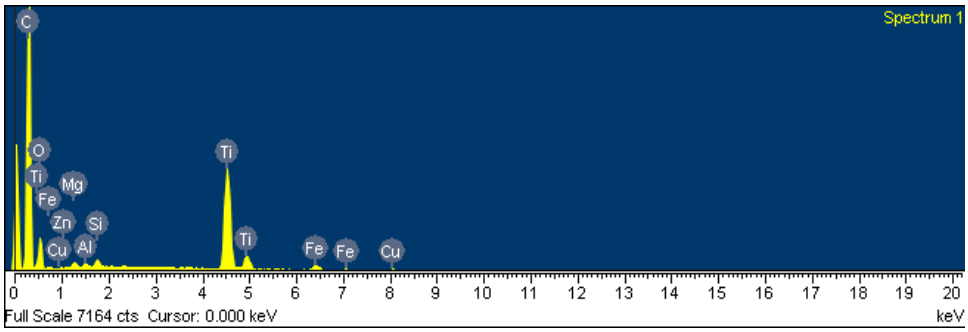

(a)

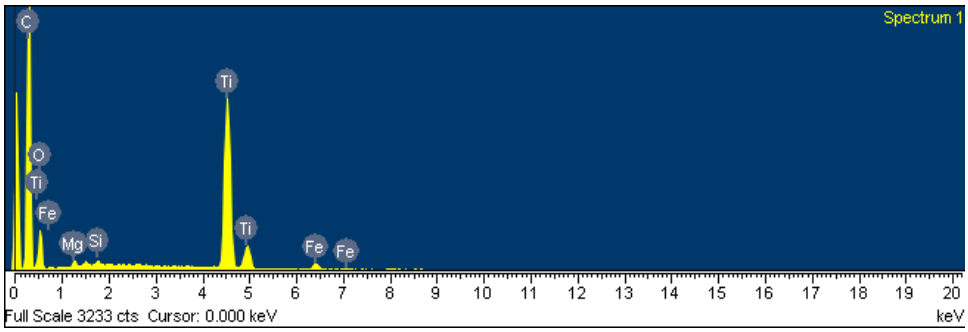

(b)

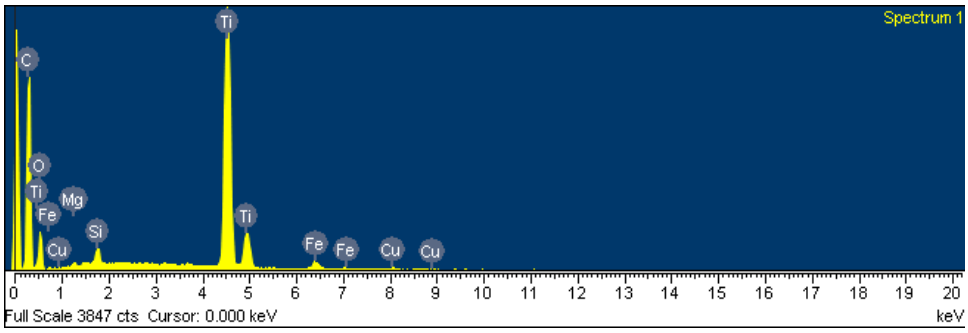

(c)

Fig. 5. EDX elemental microanalysis of CNT/TiO_2 composites: (a) SCTE1, (b) SCTE2 and (c) SCTE3

TABLE-3
EDX ELEMENTAL MICROANALYSIS OF CNT/TiO_2 ELECTRODE

Sample	C	O	Ti	Other	Total
SCTE 1	60.8	20.9	15.0	3.3	100
SCTE 2	53.4	23.0	21.7	1.9	100
SCTE 3	43.5	22.5	30.6	3.4	100

Catalytic activities: Fig. 6 shows a comparison of PC and PEC efficiency among SCTE1, SCTE2 and SCTE3 under UV irradiation with and without an electron current. The changes in relative concentration (c/c_0) of the CNT/ TiO_2 composites in the MB concentration of 1×10^{-5} mol/L under UV irradiation with and without an electron current in the aqueous solution are shown in Fig. 6. From the present results in Fig. 6, one can observe that the PC degradation efficiency of sample SCTE3 is higher than that of sample SCTE1 and SCTE2 at the same irradiation time. According to former studies[12-16], the Ti content of SCTE3 is the highest among the three samples; we can consider that the SCTE3 will have better PC degradation of the MB solution than that of the SCTE1 and SCTE2. From the results of EDX analysis, among the three types of CNT/TiO_2 composites, the SCTE3 has the lowest content of carbon and the highest content of Ti. It is considered that a decrease of the MB concentration in the aqueous solution can occur in two physical phenomena such as adsorption by CNT and PC decomposition by TiO_2.

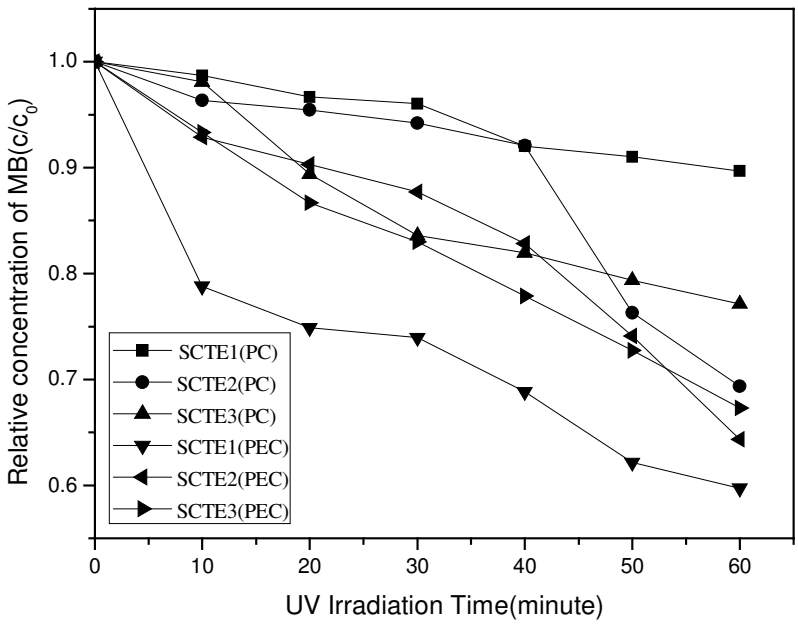

Fig. 6. Dependence of the relative concentration of MB in aqueous solutions c/c_0 on time with UV irradiation for different CNT/TiO_2 electrodes: (a) PC (UV irradiation using the electrodes without the applied potential); (b) PEC (UV irradiation using the electrodes with the applied potential 6.0 V).

For PEC degradation, the PEC degradation efficiency of sample SCTE1 is higher than that of samples SCTE2 and SCTE3 at the same irradiation time. It was possible that the PEC oxidation increased with an increase of the CNT content, the carbon content of SCTE1 is the highest among the three samples, so the CNT electro-assisted

effect of SCTE1 is better than that of SCTE2 and SCTE3. According to the literature[16,23], it is possible that the catalytic decomposition of the MB solution could be attributed to the combined effects between TiO_2 PC oxidation and CNT electro-assisted. Moreover, it is observed that the PEC effects for all samples are higher than that of the PC effect. This evidently indicates that there are two degradation types for MB: the electro-assistant activity of CNT and the PC performance of TiO_2. So the efficiency of PEC oxidation for MB is higher than that for PC oxidation.

Degradation mechanism analysis: The experimental results presented and analyzed above are indicative of the great potential of the CNT/TiO_2 composite electrodes for PEC applications. The proposed degradation processes can be expressed in three parts by the following equations[24-26]:

$$TiO_2 + hv \longrightarrow e^-_{cb} + h^+_{vb} \quad (1)$$

$$e^-_{cb} + h^+_{vb} \longrightarrow \text{heat} \quad (2)$$

$$e^-_{cb} + CNTs \longrightarrow CNTs(e^-) \quad (3)$$

$$(O_2)_{ads} + CNTs(e^-) \longrightarrow (O_2^{\bullet -})_{ads} \quad (4)$$

$$e^-_{cb} / h^+_{vb} \xrightarrow{\text{potential}} e^-_{cb} + h^+_{vb} \quad (5)$$

$$h^+_{vb} + (H_2O)ads \longrightarrow HO^\bullet + H^+ \quad (6)$$

$$h^+_{vb} + (HO^-)_{ads} \longrightarrow HO^\bullet \quad (7)$$

$$I + MB \longrightarrow I\text{--}MB \quad (8)$$

(I: adsorption site)

$$I\text{--}MB + HO^\bullet \longrightarrow I + \text{aliphatic compounds}$$

$$CO_2 + H_2O + \text{inorganic ions} \xleftarrow{HO^\bullet} \xleftarrow{HO^\bullet} \quad (9)$$

Process I: Photo-degradation of TiO_2: Under UV illumination, the excited high-energy states of e/h^+ pairs are formed in TiO_2 particles (eqn. 1). A portion of these pairs recombine in the bulk of the semiconductor (eqn. 2), while the rest migrate to the surface of the particles. An electron can be transferred from TiO_2 to CNT (eqns. 3 and 4). As more electrons are transferred from TiO_2 to CNT, the e/h^+ recombination is further reduced, more oxygens reacted with electrons in CNT to yield excited $HO^\bullet$ radicals. On the other hand, the electrons from the photon-

induced electron-hole separation process must also be removed from the TiO_2 phase, in the absence of a potential. This removal can be achieved *via* an oxidant, *e.g.* adsorbed oxygen molecules from the solution.

Process II: Electro-assistant of CNT: Multi-walled carbon nanotubes (MWCNTs) acting as an electron sensitizer and donator in a composite photocatalysts may accept an electron (e^-) induced by light irradiation. The electrons in MWCNTs may be transferred into the conduction band in the TiO_2 particles. It is considered that photo-induced charge transfer occurs in the electronic interaction between the carbon layers or walls of MWCNTs and TiO_2. The electrons formed by the light irradiation on the surface of MWCNTs migrate to the surface of TiO_2 and thus they lead to a higher rate of reduction of the e/h^+ pair recombination and increase the photon efficiency, which reduces the quantum yield of the TiO_2 catalyst. It has been confirmed that photo- or electro-induced charge transfer occurs in the electronic interaction between polymer chains and CNTs[27]. Since they connect well with each other and there is a strong interaction between CNTs and TiO_2, it can be proposed that e^- transfer also occurs in CNT/TiO_2 composites, leading to the e^-/h^- recombination and an increase of the photon efficiency. The light absorption capability of the photocatalyst and separation of photogenerated e^-/h^- pairs are crucial factors influencing the photoactivity. Accordingly, it is more reasonable to suggest that electron absorptionability of CNT/TiO_2 composites is greatly increased due to more active sites available on the CNTs surfaces. Considering the semiconducting property of CNTs, they may absorb the irradiation and inject the photo- or electro-induced electrons into the TiO_2 conduction band. These electrons in the conduction band may react with O_2, which can trigger the formation of very reactive superoxide radical ions ($O_2^{\bullet -}$) (eqns. 3 and 4). Simultaneously, a positively charged hole (h^+) might be formed with electron transfer from the valence band in TiO_2 to the CNTs. The positively charged hole (h^+) may react with the OH^- derived from H_2O, which can be produced from the hydroxyl radical ($HO^{\bullet}$). The more hydroxyl groups on the surface of photocatalysts, the more hydroxyl radicals ($HO^{\bullet}$) will be produced by the oxidation of h^+ (eqns. 6 and 7).

Process III: Function of the applied potential: In the CNT/TiO_2 composite electrodes, electrons are transferred from the TiO_2 phase (low electron conductivity) into the carbon phase (high electron conductivity). This process must overcome the interfacial resistance, which is largely fixed by the properties of the two solid phases. Therefore, to enable electron transfer, a sufficient or higher anodic potential is needed. Furthermore, the presence of an electronic conductor (CNT) dispersed through the TiO_2 phase allows a local potential difference across the TiO_2 phase to be developed throughout the sample, resulting in more effective e/h^+ separation within the entire sample. In present case, the applied potential was in the PEC, the recombination of photogenerated e/h^+ pairs was suppressed by the externally applied electric field (eqn. 5). Thus the life of the e/h^+ become longer, which hence are able to migrate to the solid-liquid interface and promote redox reactions[28,29].

Since OH^- and H_2O are the most abundant adsorbates, it is likely that holes will react with these species and then form the $HO^\bullet$ radicals, which possess a high oxidative potential, it can oxidize most organic pollutants into inorganic materials. These extremely powerful oxidizing agents can nonselectively attack the adsorbed organic molecules or those close to the catalyst surface, thus, resulting in their mineralization. Obviously, the holes are removed *via* their reaction with the MB in the solution, which however occurs only at those TiO_2/solution interfaces that are accessible to the MB molecules and this process can also be affected by mass transfer to the (MB) and from (MB oxidation product) the interface. The photo catalytic reaction occurs while both the $HO^\bullet$ radical and MB molecule are adsorbed (eqns. 8 and 9). According to this mechanistic approach, the MB molecule is decomposed into some aliphatic compounds, thus resulting in their mineralization.

Based on the experimental findings and the analysis above, it was found that photoelectrocatalytic decomposition of MB could be attributed to the synthesized effects of photo-degradation of TiO_2, electro-assistant of CNT and function of the applied potential. Thus it may be conclude that this degradation mechanism analysis is suitable to explain the results of the PEC degradation of methylene blue using the prepared CNT/TiO_2 composite electrodes.

Conclusion

In this study, we presented the fabrication and characterization of CNT/TiO_2 composite electrodes. The BET surface areas for CNT/TiO_2 composites decreased with an increase of the TNB component. XRD data revealed that the structure for the SCTE1 showed a typical single and clear anatase crystal structure. However, with an increase of TNB the structure for SCTE2 and SCTE3 showed a mixture of anatase and rutile crystals. The SEM micrographs of CNT/TiO_2 composites showed that TiO_2 particles were fixed on the surface of the CNT network in the forms of small clusters and that the distribution was not uniform. From the EDX data, the main elements of C, O and Ti were shown to exist. The photodegradation of MB using the prepared electrode under different experimental conditions was investigated in terms of UV absorbance. The results demonstrated that the PEC oxidation of the MB concentration in an aqueous solution can be attributed to the combined effects of PC decomposition by TiO_2, CNT network electro-assisted and the function of the applied potential. Comparing the PC oxidation and PEC oxidation, the efficiency of the PEC oxidation for MB is higher than that of PC oxidation.

REFERENCES

1. M.R. Hoffmann, S.T. Martin, W.Y. Choi and D.W. Bahnemann, *Chem. Rev.*, **95**, 69 (1995).
2. A.K. Ray, *Chem. Eng. Sci.*, **54**, 3113 (1999).
3. P.F. Fu, Y. Luan and X.G. Dai, *J. Mol. Catal. A: Chem.*, **221**, 81 (2004).
4. Z. Ding, X.J. Hu, P.L. Yue, G.Q. Lu and P.F. Greenfield, *Catal. Today*, **68**, 173 (2001).
5. X.Z. Li, H.L. Liu and P.T. Yue, *Environ. Sci. Technol.*, **34**, 4401 (2000).
6. F.Y. Oliva, L.B. Avalle, E. Santos and O.R.C´amara, *J. Photochem. Photobiol. A: Chem.*, **146**, 175 (2002).

7. G. Colon, M.C. Hidalgo and J.A. Navio, *Appl. Catal. B: Environ.*, **45**, 39 (2003).
8. P.A. Christensen, T.P. Curtis, T.A. Egerton, S.A.M. Kosa and J.R. Tinlin, *Appl. Catal. B: Environ.*, **41**, 371 (2003).
9. X.Z. Li, F.B. Li, C.M. Fan and Y.P. Sun, *Water Res.*, **36**, 2215 (2002).
10. D.L. Jiang, H.J. Zhao, S.Q. Zhang and R. John, *J. Catal.*, **223**, 212 (2004).
11. L. Zhang, Y.F. Zhu, Y. He, W. Li and H.B. Sun, *Appl. Catal. B: Environ.*, **40**, 287 (2003).
12. M.L. Chen, J.S. Bae and W.C. Oh, *Carbon Sci.*, **7**, 259 (2006).
13. M.L. Chen, J.S. Bae and W.C. Oh, *Bull. Korean Chem. Soc.*, **27**, 1423 (2006).
14. M.L. Chen, J.S. Bae and W.C. Oh, *Anal. Sci. Technol.*, **19**, 376 (2006).
15. M.L. Chen, Y.S. Ko and W.C. Oh, *Carbon Sci.*, **8**, 6 (2007).
16. W.C. Oh, A.R. Jung and W.B. Ko, *J. Ind. Eng. Chem.*, **13**, 1208 (2007).
17. W.C. Oh and M.L. Chen, *Bull. Korean Chem. Soc.*, **29**, 159 (2008).
18. M. Inagaki, Y. Hirose, T. Matsunaga, T. Tsumura and M. Toyoda, *Carbon*, **41**, 2619 (2003).
19. W.C. Oh and M.L. Chen, *J. Ceram. Process. Res.*, **9**, 100 (2008).
20. W.D. Wang, P. Serp, P. Kalck, C.G. Silva and J.L. Faria, *Mater. Res. Bull.*, **43**, 958 (2008).
21. W.D. Wang, P. Serp, P. Kalck and J.L. Faria, *J. Mol. Catal. A: Chem.*, **235**, 194 (2005).
22. D. Jiang, H. Zhao, S. Zhang and R. John, *J. Catal.*, **223**, 212 (2004).
23. F.J. Zhang, M.L. Chen and W.C. Oh, *Mater. Res. Soc. Korea*, **18**, 583 (2008).
24. J.S. Chen, M.C. Liu, L. Zhang, J.D. Zhang and L.T. Jin, *Water Res.*, **37**, 3815 (2003).
25. C.Y. Kuo, *J. Hazard. Mater.*, **163**, 239 (2009).
26. E. Bizani, K. Fytianos, I. Poulios and V. Tsiridis, *J. Hazard. Mater.*, **136**, 85 (2006).
27. Y. Yu, J.C. Yu, J.G. Yu, Y.C. Kwok, Y.K. Che, J.C. Zhao, L. Ding, W.K. Ge and P.K. Wang, *Appl. Catal. A. Gen.*, **289**, 186 (2005).
28. M.J. O'connell, Carbon Nanotubes Properties and Applications, CRC Press, USA (2006).
29. B. Gao, C. Peng, G.Z. Chen and G.L. Puma, *Appl. Catal. B: Environ.*, **85**, 17 (2008).

(*Received*: 13 October 2009; *Accepted*: 26 March 2010) AJC-8571